ORIGINAL PAPER

Research on Energy Characteristics of Shaft Blasting Vibration Based on Wavelet Packet

Wei Wang · **Liangjun Song · Quanwei You ·
Xudong Zheng**

Abstract Analyzing the time–frequency and energy variation characteristics of blasting vibration signals is helpful to understand the propagation law of blasting seismic waves and guide the optimization of blasting parameters. The study is based on the field-measured tunnel shaft blasting vibration signal data and uses wavelet packets to extract the energy frequency band characteristics of the vibration signal. The distribution of blasting vibration signal energy in each frequency band and the change law with vertical distance are analyzed, and the regression analysis of shaft blasting vibration energy is carried out according to the principle of dimensional analysis. The results show that the main frequency band of the shaft blasting vibration signal is distributed within 0–300 Hz, and the variation trend of blasting vibration energy in different frequency bands is different. The results show that the vibration energy of shaft blasting accounts for 99% of the energy in the 0–300 Hz frequency band, and the vibration energy in the vertical direction accounts for the most. The energy is concentrated in the low frequency band, and the average proportion of energy in the frequency range of 0–30 Hz at 25 m, 31 m, and 41 m from the explosion source is 86.21%, 49.67%, and 39.10%, which is not conducive to the safety of structures. The energy attenuation coefficient of the shaft is about twice that of the tunnel, and seismic wave propagation has an elevation amplification effect.

1 Introduction

With the rapid progress of production capacity and technology, tunnel construction is gradually developing into construction projects with high technical requirements such as long and large tunnels and complex geological tunnels (Zhang et al. 2018; Shi et al. 2021). The shafts of extra-long highway tunnels are continuously included in the construction planning, which is related to the scale of the tunnel project, construction period, post-operation costs, and disaster prevention and rescue (Yao et al. 2019; Cong et al. 2021; Wang et al. 2023). The vertical excavation of the shaft is different from the tunnel excavation process. The blasting vibration has an amplification effect in the elevation direction, and the internal blasting vibration attenuation law is affected by the unique spatial geometry and constraints. It is different from the law of blasting vibration propagation in continuous geology and tunnel lateral excavation (Li et al. 2018; Ma et al. 2021; Xie et al. 2022). In the process of shaft excavation, the construction method combining mechanical construction with the drilling and blasting method is generally adopted. As an

W. Wang (✉) · L. Song · Q. You · X. Zheng
Central South University, Changsha, Hunan, China
e-mail: wangweicsu@csu.edu.cn

efficient rock-breaking technology commonly used in production and construction, the drilling and blasting method has an efficient rock-breaking ability, which improves the efficiency of engineering construction and reduces the labor intensity of workers, which makes blasting technology more and more used in the field of engineering construction (Yang et al. 2020; Huang et al. 2015; Afum et al. 2015; Pomasoncco et al. 2022). With the development of refined construction processes, higher requirements are put forward for shaft blasting construction technology. Unreasonable blasting construction technology will enhance the direct damage and cumulative damage effect of the shaft wall and the existing lining and even lead to direct damage to the shaft wall, which increases the construction cost and also brings great security risks (Ding et al. 2021; Li et al. 2014; Xue et al. 2016; Khademian et al. 2019; Xie et al. 2019).

To observe the impact of blasting on surrounding rock and buildings, blasting vibration signals are usually collected for analysis. The propagation law of blasting seismic waves can be obtained by analyzing the blasting vibration signal and then guides the optimization of blasting construction (Wu et al. 2022a, b; Wenbin et al. 2015). The impact of blasting vibration on buildings can be regarded as the process of energy transfer and transformation. In terms of the mechanism of building damage caused by earthquakes, there are also vibration damage mechanisms and seismic design methods based on the concept of energy (Agrawal et al. 2018; Agrawal et al. 2022; Ling et al. 2023). The energy reflects the strength of the blasting vibration, and the damage to the tunnel is more intuitive. The frequency of the blasting vibration signal is also the main factor that threatens and destroys the stability of buildings (Mehboob et al. 2022; Wang et al. 2022; Zhang et al. 2020). The blasting vibration signal is characterized by instantaneous, sudden change and oscillation, which is a typical non-stationary signal. Time–frequency analysis technology has become an important means to deal with such non-stationary signals (Chen et al. 2019). Commonly used blasting vibration signal analysis methods include Fourier transform, short-time Fourier transform, wavelet and wavelet packet transform, etc. (Libal et al. 2014; Xu and Deng 2016; Ainalis et al. 2018; Huang et al. 2019; Ma et al. 2023). Fourier transform can convert time-domain signals to frequency-domain signals for analysis, but Fourier transform does not have any time-domain signals. For non-stationary and nonlinear signals that lack local information, local analysis of signals cannot be performed (Robustelli et al. 2018; Tyrtaiou et al. 2020). The short-time Fourier transform expresses the signal characteristics at a certain moment through a section of the signal in the time window and realizes the problem of local analysis of the Fourier transform. The accuracy of time and frequency depends on the length of the window function. The wider the window, the better the frequency resolution, but the worse the time resolution (Jing et al. 2018; Khodja et al. 2019). Wavelet transform is adaptive to signals, which overcomes the shortcomings of Fourier transform that cannot be localized in time and frequency domains. The wavelet packet analysis further improves and perfects the wavelet analysis, and divides the signal more finely. It can refine and decompose the high-frequency part of the signal, and divide the signal frequency band into multi-level divisions, and adaptively select the best wavelet basis functions. The research of many experts and scholars shows that the wavelet packet analysis method can effectively decompose the blasting vibration signal and obtain accurate frequency and energy characteristics of the blasting vibration signal (Schimmack 2019; Tian et al. 2019; Pak et al. 2022; Wu et al. 2022a, b).

However, because the blasting vibration response and propagation law vary with engineering geology, topography, and structural form characteristics, the existing research results do not fully understand the vibration response characteristics of tunnel shaft blasting construction. There are not many research results on the evolution mechanism of vibration energy under blasting excavation of tunnel shaft excavation. Therefore, this paper takes a shaft project as the research background, uses the wavelet packet method to analyze the energy frequency band characteristics of the measured blasting vibration signal, and reveals the blasting vibration energy propagation and attenuation law and the impact of blasting distance on the blasting vibration frequency band energy. The research rules can provide a reference for the construction optimization of similar shaft blasting projects.

Table 1 Shaft blasting parameters

Detonation sequence	Number of holes	Hole depth (m)	Hole spacing (cm)	Single hole charge (Kg)
No. 1	12	2.5	79	1.8
No. 2	19	2.2	80	1.5
No. 3	40	1.6	50	0.9

2 Engineering Background

2.1 Blasting Construction

The shaft project is located in the Shaoxing-Jinhua TJ-08 bid section of the Hangshaotai Expressway, and the mileage range of the bid section is K91+600~101+700. In order to meet the ventilation requirements for the operation of extra-long tunnels, the pilot hole of the shaft was excavated using the raised drilling rig construction method, and the excavation was formed by forward blasting. The inner outline of the tunnel shaft has a clear width of 6.4 m, the elevation at the bottom of the shaft is 128.8 m, and the total length of the shaft is 226.2 m. The excavation of the bedrock section of the shaft adopts the straight hole cutting blasting method, without coupling the charge structure. A drilling rig was used to drill holes, gradually reducing the amount of charge from the center to the outside, the hole diameter was 42 mm, and φ32 mm emulsion explosive was used. Three rows of blast holes were arranged in the test. The blasting parameters are shown in Table 1.

2.2 Monitoring Program

When the shaft is excavated, it is difficult to directly fix the detection instrument on the shaft wall due to the narrow working face and large longitudinal depth of the shaft excavation. Therefore, the reserved steel pipe fittings are welded to the shaft wall steel frame and embedded in the concrete before the lining is constructed on-site to ensure the reliability of the reserved measuring points. The pre-buried fixed monitoring instrument is at a depth of 65 m from the surface of the shaft, and the three-way velocity

sensor is fixed in the steel pipe through gypsum to ensure that the z direction is vertically upward and the x direction is consistent with the direction of the shaft diameter. Considering that the impact force of the actual blasting is relatively large, the broken flying rocks may damage the sensing wire and cause the test to fail. The sensing wire in the well is wrapped with a custom-made thickened sensing wire casing to protect it from impact damage. The sensing line is connected with the sensor fixed in the shaft and extends out of the ground along the shaft wall to connect with the vibration meter. In order to ensure the safety of monitoring personnel when collecting data, the sampling time and trigger level are set. The monitoring point is located in the medium-weathered basalt formation, and the surrounding rock at the blasting face is medium-weathered tuff, at a depth of 90 m from the surface of the shaft. During this monitoring process, the positions of the measuring points remained unchanged. The corresponding monitoring data obtained with the advancement of the face is shown in Table 2. Nine groups of blasting vibration test results without abnormal data were selected for analysis (Figs. 1, 2).

3 Principle of Wavelet Packet

Wavelet analysis has poor time resolution in the low-frequency band and poor frequency resolution in the high-frequency band, while wavelet packet analysis can divide the frequency band into multiple levels, and can decompose the low-frequency and high-frequency parts of the signal at the same time, which is a more refined signal analysis method. Wavelet packet analysis can adaptively select the frequency band according to the characteristics of the signal to improve the time–frequency resolution, which is more suitable for the analysis of non-stationary signals such as blasting vibration signals. After the wavelet packet decomposition of the blasting vibration signal $s(t)$, the subspace signals on 2^i frequency bands can be obtained, then $s(t)$ can Research on Energy Characteristics of Shaft Blasting Vibration Based on Wavelet Packet be expressed as:

Table 2 Blasting vibration monitoring data

Measuring point	Peak vibration velocity (cm/s)				Distance (m)	Segment maximum dose/kg
	x	y	z	Vibration velocity		
1	0.796	0.941	2.565	2.846	25	23.1
2	0.779	0.733	2.496	2.716	27	23.1
3	0.724	0.434	2.339	2.487	29	23.1
4	0.267	0.012	2.162	2.178	31	23.1
5	0.010	0.404	2.207	2.244	33	23.1
6	0.801	0.682	1.539	1.865	35	23.1
7	0.396	0.345	1.254	1.360	37	23.1
8	0.466	0.571	1.122	1.342	39	23.1
9	0.486	0.426	1.331	1.480	41	23.1
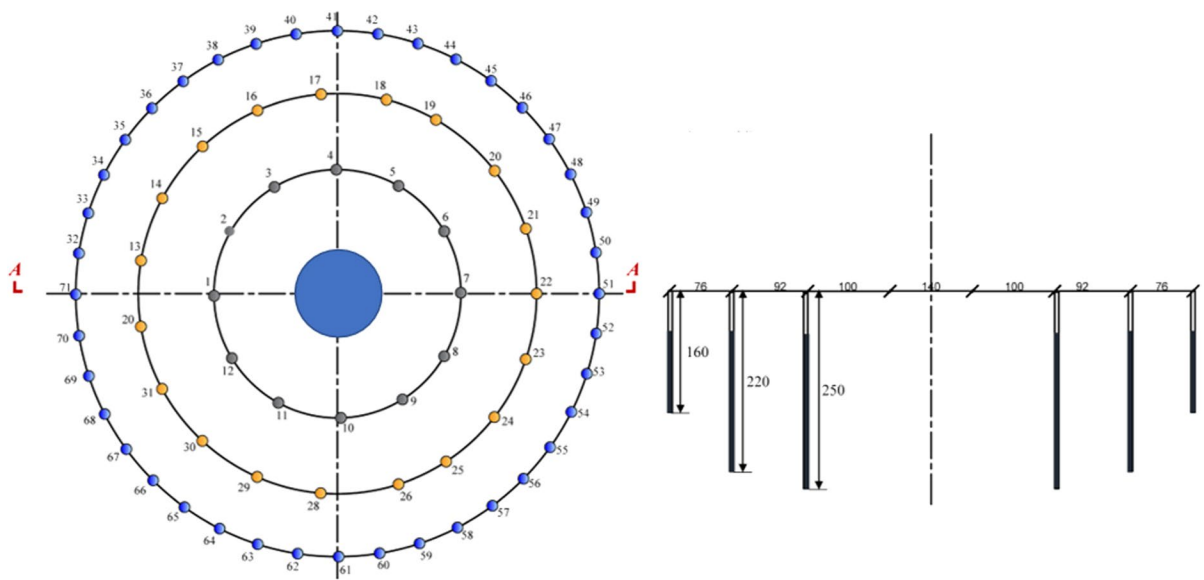
**Fig.1** Schematic diagram of vertical shaft blast hole layout

$$s(t) = \sum_{j=0}^{2^i-1} f_{i,j}(t_j) = f_{i,0}(t_0) + f_{i,1}(t_1) + \cdots + f_{i,2^i-1}(t_{2^i-1}), \quad j = 0, 1, 2, \ldots, 2^i - 1 \tag{1}$$

In the formula, $f_{i,j}(t_j)$ is the reconstructed signal from the wavelet packet decomposition of the blasting vibration signal to the decomposition node (i, j) of the i-th layer. If the frequency width of the signal $s(t)$ is ω, then the frequency width of each sub-band in the i-th layer is $\omega/2^i$. According to the Parseval theorem in signal spectrum analysis (Baumgart et al. 2022; Maher et al. 2022), the energy spectrum of blasting vibration signal $s(t)$ wavelet packet analysis can be obtained from formula (1):

$$E_{i,j} = \int_T \left\| f_{i,j}(t_j) \right\|^2 dt = \sum_{k=0}^{m} |x_{j,k}|^2 \tag{2}$$

In the formula: $x_{j,k}$ are the amplitudes of the discrete points of the reconstructed signal;
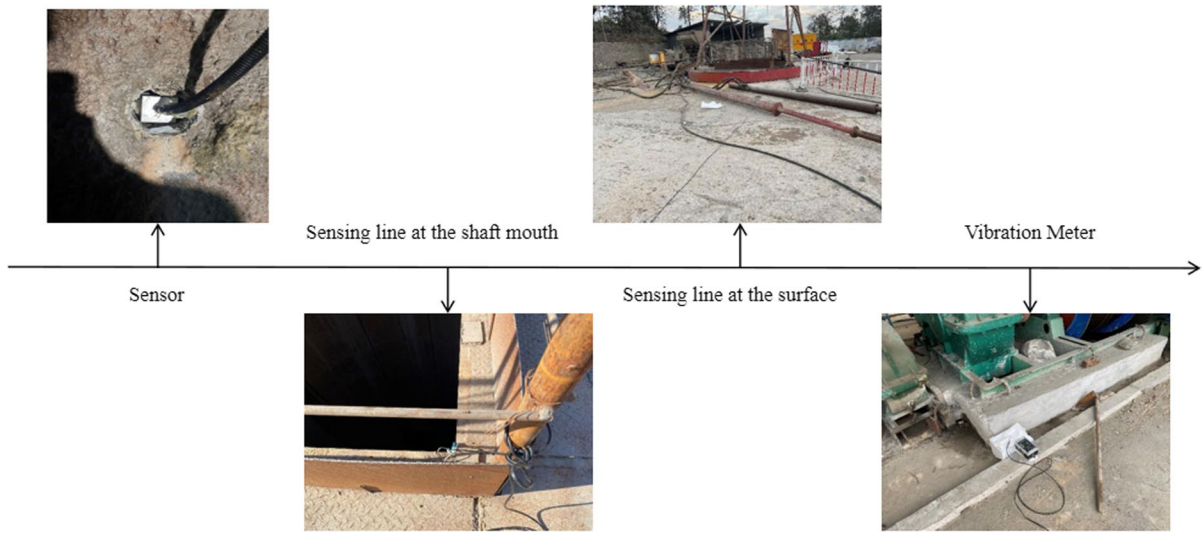
Fig. 2 Layout of on-site vibration measuring instruments

$j = 0,1,2,\cdots,2^i$-1; $k = 0,1,2, \cdots, m$; m is the blasting vibration The number of signal sampling points. The total energy E_0 of the signal and the percentage $P_{i,j}$ of the energy of each sub-band to the total energy of the signal can be expressed as:

$$E_0 = \sum_{j=0}^{2^i-1} E_{i,j} \qquad (3)$$

$$P_{i,j} = \frac{E_{i,j}}{E_0} \qquad (4)$$

The TC-4850 vibrometer was used for the blasting test, the sampling frequency was 2500 Hz, and the Nyquist frequency was 1250 Hz. 8-layer wavelet decomposition was performed on the blasting vibration signals of each measuring point, and a total of 28 sub-frequency bands were generated, and the decomposition frequency bandwidth was 4.883 Hz. In this paper, the error analysis of the wavelet function commonly used in the analysis of blasting vibration signals is carried out. It can

be seen from Table 3 that the experimental data is based on the sym5 wavelet base time, the reconstruction peak error between the original signal and the reconstructed signal is the smallest, and the reconstruction accuracy is the highest. Therefore, the sym5 wavelet base is selected as the optimal wavelet base for this experiment.

4 Energy Distribution Characteristics of Shaft Blasting Vibration Signal

4.1 Analysis of Frequency Band Distribution of Blasting Vibration Signal Energy

According to the blasting earthquake safety energy analysis method based on wavelet transform proposed by Zhong et al. (2006), the relationship between the characteristic frequencies of different frequency bands of blasting earthquake signals and the natural vibration frequency of controlled buildings will affect the buildings affected by blasting earthquakes. When the blasting vibration energy is concentrated in the

Table 3 Wavelet reconstruction deviation values

Wavelet base type	db3	db5	db8	sym5	sym7
Deviation	$2.253e^{-11}$	$6.264e^{-12}$	$1.023e^{-11}$	$5.753e^{-13}$	$2.371e^{-12}$

low-frequency band, it is not good for the project. Therefore, analyzing the distribution of energy in each frequency band will help technicians to adjust the blasting parameters and reduce vibration. The Matlab wavelet packet energy analysis code is compiled to extract the energy features calculated from wavelet packets of measurement points 1~3, and the energy distribution of each frequency band of the shaft blast vibration signal is calculated as shown in Table 4.

It can be seen from Table 4 that the energy distribution range of the shaft blasting vibration signal is relatively concentrated. Taking the No. 1 measuring point as an example, the energy in the frequency band of vibration velocity 0–300 Hz in the x direction accounts for 98.90% of the total energy; The ratio of the energy in the 300 Hz frequency band to the total energy is 98.70%; the ratio of the energy in the 0–300 Hz frequency band of the z-direction vibration

Table 4 Frequency band energy distribution of vibration signals at measuring points 1, 2, and 3

frequency band (Hz)	Measuring point 1			Measuring point 2			Measuring point 3		
	x	y	z	x	y	z	x	y	z
0~4.883	13.849	30.576	41.29	8.890	22.192	24.551	6.592	18.160	8.896
4.883~9.766	41.288	71.852	44.921	6.917	24.48	13.070	8.660	42.664	8.441
9.766~14.649	62.974	187.69	235.46	17.135	7.036	15.231	9.932	34.808	93.186
14.649~19.532	15.634	129.16	356.48	9.718	1.795	6.801	15.664	11.056	248.78
19.532~24.415	3.913	35.47	345.60	2.756	1.530	7.272	2.873	4.446	283.80
24.415~29.298	9.008	17.922	180.08	4.109	0.502	106.71	18.266	4.607	79.530
29.298~34.181	10.263	5.081	79.947	5.155	0.747	70.971	16.090	1.118	119.69
34.181~39.064	5.522	1.660	41.794	0.640	0.232	10.982	19.162	0.999	88.824
39.064~43.947	4.662	1.102	27.695	1.260	0.216	27.203	14.125	1.140	59.45
43.947~48.83	2.391	1.421	17.70	0.462	0.131	23.964	4.883	0.495	44.479
48.83~53.713	3.824	0.643	18.143	0.248	0.084	0.713	5.907	0.302	15.408
53.713~58.596	0.503	0.375	2.702	0.024	0.016	1.075	0.604	0.143	11.191
58.596~63.479	0.286	0.188	1.544	0.116	0.014	0.176	0.728	0.091	3.892
63.479~68.362	0.151	0.083	0.389	0.015	0.008	0.166	0.519	0.033	1.926
68.362~73.245	0.063	0.037	0.351	0.039	0.010	0.095	0.786	0.031	0.880
73.245~78.128	0.060	0.020	0.133	0.018	0.003	0.073	0.228	0.009	0.479
78.128~83.011	0.093	0.019	0.219	0.010	0.002	0.221	0.214	0.014	0.489
83.011~87.894	0.031	0.017	0.150	0.007	0.002	0.130	0.156	0.012	1.143
87.894~92.777	0.035	0.010	0.330	0.016	0.003	0.053	0.376	0.014	0.796
92.777~97.66	0.069	0.027	0.173	0.015	0.003	0.154	0.060	0.026	0.566
97.66~102.543	0.044	0.016	0.213	0.012	0.003	0.018	0.065	0.007	0.330
102.543~107.426	0.024	0.006	0.184	0.011	0.003	0.027	0.065	0.014	1.170
107.426~112.309	0.022	0.009	0.097	0.009	0.001	0.084	0.162	0.004	0.386
112.309~117.192	0.026	0.013	0.221	0.005	0.002	0.053	0.088	0.005	0.356
117.192~122.075	0.029	0.005	0.149	0.010	0.003	0.128	0.058	0.008	0.325
122.075~126.958	0.013	0.007	0.060	0.007	0.002	0.101	0.022	0.002	0.198
126.958~131.841	0.014	0.003	0.066	0.005	0.002	0.004	0.014	0.001	0.039
131.841~136.724	0.003	0.001	0.007	0.003	0.002	0.002	0.002	0.001	0.030
136.724~141.607	0.001	0.001	0.003	0.003	0.002	0.002	0.003	0.001	0.012
141.607~146.49	0.001	0.000	0.001	0.003	0.002	0.002	0.001	0.000	0.003
146.49~151.373	0.001	0.000	0.001	0.004	0.003	0.002	0.001	0.000	0.001
151.373~200.203	0.012	0.005	0.005	0.037	0.026	0.026	0.009	0.005	0.011
200~300	0.017	0.007	0.022	0.043	0.020	0.024	0.028	0.014	0.051
0~1250	174.98	483.58	1396.3	57.79	57.180	310.21	126.47	120.35	1074.9

velocity to the total energy is 99.10%, and the main frequency band of blasting vibration is distributed within 0–300 Hz. In the shaft blasting vibration energy, the z-direction vibration energy accounts for the largest proportion, accounting for 67.95% of the total blasting vibration energy. The frequency range of shaft blasting vibration energy is 0–60 Hz. The main frequency of blasting vibration plays a vital role in the surrounding rock and lining structure. The proportion of energy in the frequency band above 300 Hz is too low, and the impact of this part on the structure can be ignored in the study. The role of stability. Taking the data of measuring point No. 1 as an example, the frequency bands within 0–300 Hz are segmented according to 0–60, 60–120, 120–180, 180–240, and 240–300 Hz.

The natural vibration frequency of engineering structures is low. When the energy generated by blasting vibration is distributed in the low frequency band, the blasting earthquake will have a greater impact on the structure, which is not conducive to the safety of buildings. It can be seen from Fig. 3 that the energy distribution in the x and y directions is uniform, while the blasting vibration energy in the shaft direction spreads to adjacent areas, which may affect nearby buildings, equipment, and underground pipelines. Attention should be paid to vertical vibration reduction measures in vertical shaft blasting vibration. In addition, the change of energy with distance also needs attention.

4.2 The Influence of Distance on the Energy Distribution of Different Frequency Bands of the Signal

In order to analyze the influence of propagation distance on the energy distribution of blasting vibration, according to the blasting vibration signal obtained from the test monitoring and the data of No. 1 to No. 6 measuring points as the research data, as shown in Fig. 4, the energy distribution is analyzed.

Since the order of magnitude difference of wavelet packet energy values in different frequency bands within the frequency range of 0–1250 Hz is too large, the energy value of blasting vibration beyond 100 Hz is small and belongs to the oscillation stage, which has no significant impact on the propagation distance law. In the frequency range of 0~100 Hz, the relationship between the blasting vibration energy and

the propagation distance in the three directions of x, y, and z is studied.

From the energy distribution of blasting vibration signals at different measuring points in Figs. 5, 6, 7, it can be seen that the energy of blasting vibration signals in the x direction increases first and then decreases with the increase of frequency, showing a negative parabolic distribution, and the blasting vibration energy is mainly concentrated at 10~60 Hz frequency range. With the increase of propagation distance, the peak time of vibration energy in the x direction is delayed, the peak value of vibration energy decreases first and then increases, and the energy changes show a local trend of moving first to the higher frequency segment and then to the lower frequency segment. The blasting vibration energy in the y direction is also distributed in a negative parabolic shape as the frequency increases, and the blasting vibration energy first increases and then decreases. With the increase of the propagation distance, the blasting vibration energy in the y direction gradually decreases with the increase of the propagation distance, the energy concentration area shows a local trend of moving to the lower frequency band first and then to the higher frequency band, and the energy distribution changes relatively steadily. The blasting vibration energy in the z direction increases first and then decreases with the increase of frequency. With the increase of propagation distance, the blasting vibration energy in the main frequency segment moves slightly backward compared with that in the x and y directions. The energy attenuation speed is faster in the range of 0~30 Hz, and then the energy attenuation is slow.

The energy peak of x and y blast vibration occurs in the frequency range of 0–30 Hz, 35 m from the explosion source, the energy peak in both directions is more than 100 cm^2/s^2. z direction blast vibration energy peak also occurs in the frequency range of 0–30 Hz, the closest to the explosion source, its energy peak is 356 cm^2/s^2. The z-direction plays a major role in energy dissipation during shaft blasting and vibration damping measures need to be done in the z-direction in places close to the palm face, while the vibration effects in the x- and y-directions need to be taken into account in distant areas of the blast.
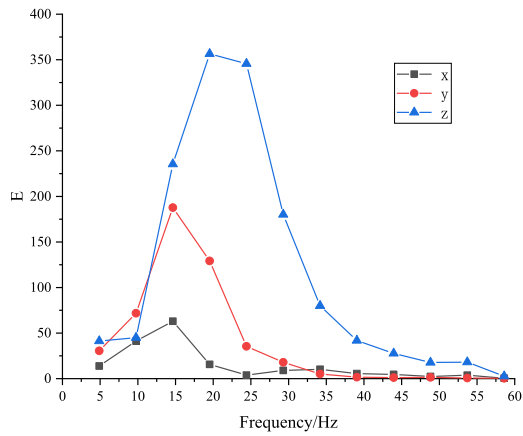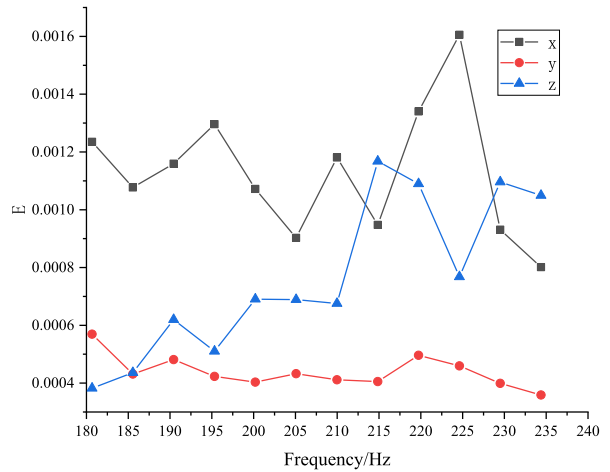
(a) Wavelet packet energy value in the
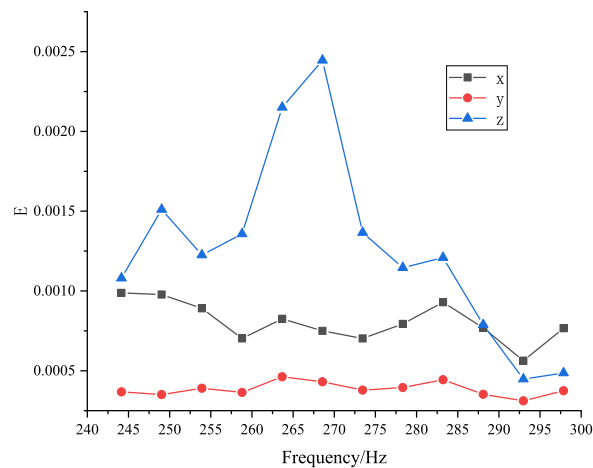frequency range of 0~60 Hz
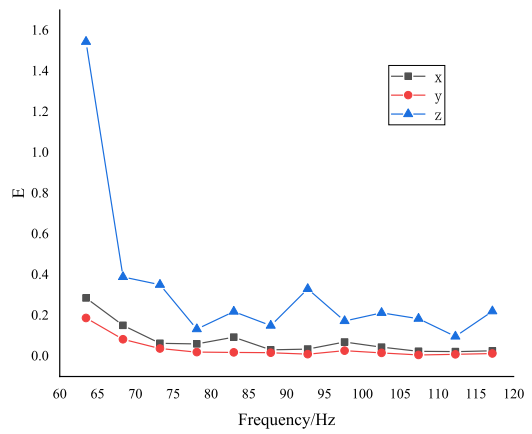
(b) Wavelet packet energy value in the frequency
range of 60~120 Hz
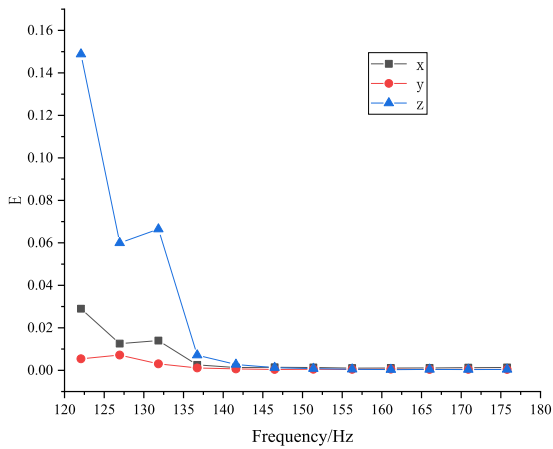
(c) Wavelet packet energy value in the
frequency range of 120~180 Hz

(d) Wavelet packet energy value in the frequency
range of 180~240 Hz

(d) Wavelet packet energy value in the frequency range of 240~300 Hz

◀**Fig. 3** Variation trend of wavelet packet energy value in each frequency band

4.3 Regression Analysis of Shaft Blasting Vibration Energy

Since the actual blasting vibration process at the shaft construction site is very complex, and the actual blasting vibration energy distribution and propagation are affected by many factors, it is difficult to know the impact of blasting vibration through direct monitoring. In the past, the energy attenuation formula derived by some scholars was used in the prediction and analysis of blasting vibration energy, and achieved good results. In this section, the regression prediction analysis of shaft blasting is carried out according to the measurement results of shaft blasting vibration.

The blasting vibration data was fitted using origin software, and the fitting results are shown in Fig. 8. The fitted Sadowski formula is shown in Eq. (5). The correlation coefficient $R^2 = 0.902$, the correlation coefficient $k = 82.36$, and the attenuation coefficient $\alpha = 1.51$ of the blasting regression characteristic curve obtained by fitting.

$$V = 82.36\left(Q^{1/3}/R\right)^{1.51} \tag{5}$$

Shaft blasting vibration energy is related to charge, explosive density, elastic modulus, propagation distance, and blasting vibration velocity. Therefore, if the above parameters are taken as the main factors of blasting vibration energy, the relationship between blasting vibration energy E and the above parameters can be expressed as:

$$f(E, Q, \rho, V, R) = 0 \tag{6}$$

According to the dimensional homogeneity theorem, functional Eq. (6) is simplified as:

$$f\left(\frac{Q}{\rho R^3}, \frac{E_0}{\rho R^3}\right) = 0 \tag{7}$$

Simplify formula (7) to extract the blasting vibration energy formula:

$$E_0 R^{-3} = K\phi(Q^{1/3}R) \tag{8}$$

In order to facilitate the study of the propagation law of blasting vibration energy attenuation, referring to the form of the Sadovsky formula, the blasting vibration energy attenuation formula is expressed as follows:

$$E^* = K(Q^{1/3}R)^{\alpha} \tag{9}$$

In the formula, $E^* = E_0 R^{-3}$, E^* is the proportional blasting vibration energy; K and α are coefficients related to rock properties.

The blasting vibration energy attenuation formula is used to perform regression fitting on the blasting vibration energy attenuation law, and the fitting results of the combined vibration velocity blasting vibration energy are shown in Fig. 9.

As the propagation distance increases, the proportional blasting vibration energy decays gradually. Regression analysis of the combined vibration velocity measurement data shows that $K = 6.34986 \times 10^4$, $\alpha = 6.064$, and the attenuation law of the total energy of shaft blasting satisfies:

$$E^* = 6.34986 \times 10^4\left(Q^{1/3}/R\right)^{6.064}, R^2 = 0.925 \tag{10}$$

Similarly, the energy attenuation formula of blasting vibration in the x, y, and z directions is shown in Eq. (11):

$$\begin{cases} E_x^* = 7.6142 \times 10^4\left(Q^{1/3}/R\right)^{4.109}, R^2 = 0.945 \\ E_y^* = 7.5063 \times 10^4\left(Q^{1/3}/R\right)^{12.125}, R^2 = 0.904 \\ E_x^* = 7.2504 \times 10^4\left(Q^{1/3}/R\right)^{6.306}, R^2 = 0.971 \end{cases} \tag{11}$$

According to the law of energy attenuation, it can be known that the law of energy attenuation in all directions is in the form of a power function, and the energy attenuates very quickly when the blasting distance is within 30 m. At this time, rock breaking and fracturing consume a lot of energy. In the range of 30–40 m, the energy attenuation rate gradually decreases with the increase of the propagation distance. The blasting vibration energy decays fastest in the y-direction, followed by the blasting vibration in the z-direction. The attenuation rate of blasting vibration energy in the x direction is slow, but the proportion of blasting vibration energy in the total energy is relatively high, indicating that there is relatively continuous energy acting in this direction, and vibration
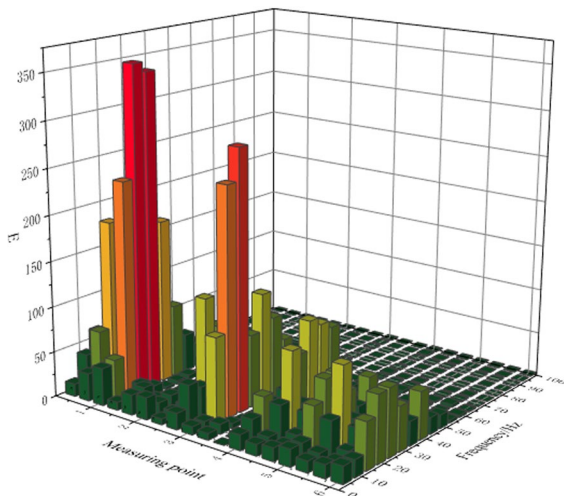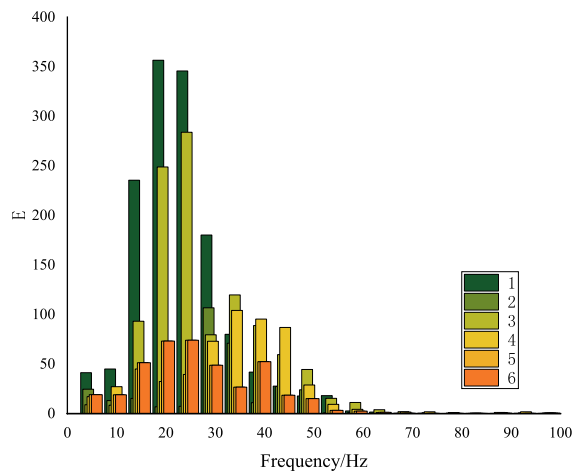
Fig. 4 Energy distribution of blasting vibration signal at measuring points
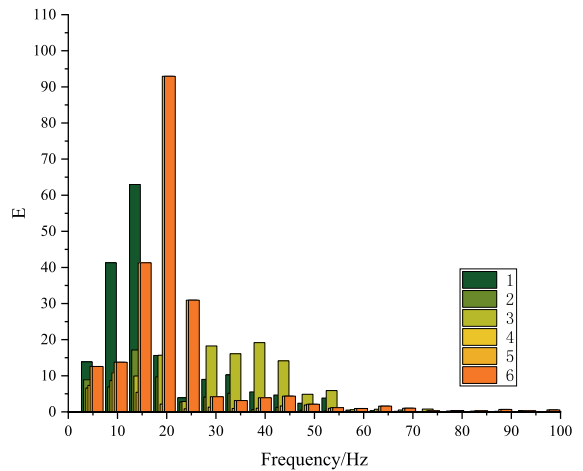
Fig. 6 Energy distribution of blasting vibration signal in y-direction
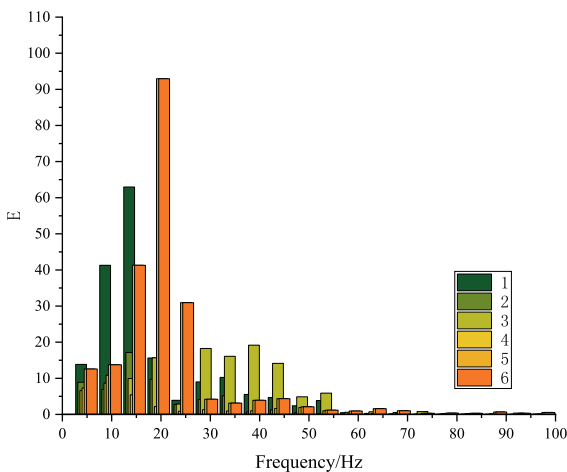
Fig. 5 Energy distribution of blasting vibration signal in x-direction

Fig. 7 Energy distribution of blasting vibration signal in z-direction

reduction measures in this direction need to be considered. The blasting vibration in the y direction will lead to shear failure of the shaft wall, but in the actual blasting, the ratio of the blasting vibration energy to the total energy is low, and the impact on the surrounding rock and structure is small, so only the damage in the near area of the blasting in the y direction needs to be considered. The ratio of blasting vibration energy to total energy in the z direction is the highest, and the energy decay rate is faster.

Some scholars have studied and compared the energy attenuation coefficient and vibration velocity attenuation coefficient of tunnel blasting and found that there is a certain multiple or power relationship between them (Shan et al. 2018). The energy attenuation formula and the vibration velocity attenuation formula of shaft blasting are obtained by regression calculation. It can be found that the energy attenuation coefficient and the speed attenuation coefficient present a multiple relationship. The energy
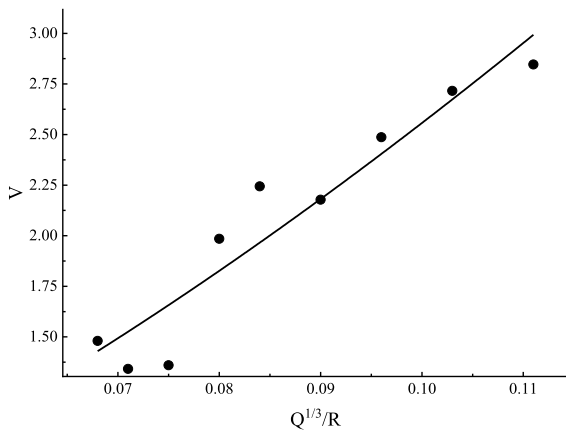
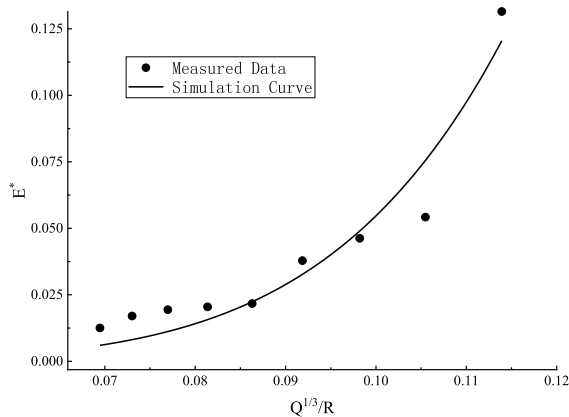**Fig. 8** Fitting curve of blasting vibration velocity

Fig. 9 Regression analysis of blasting vibration energy

attenuation coefficient K_E and the velocity attenuation coefficient K_V are not in the same order of magnitude. Compared with the existing regression analysis of tunnel blasting, the relationship between excavation energy and velocity attenuation coefficient of shaft vertical blasting is different from that of the tunnel. Referring to the research results of the blasting energy attenuation law of the Heiyu Tunnel (Song 2019), the calculated tunnel energy attenuation formula is:

$$E' = 4.256 \times 10^6 R^{-3.011} \qquad (12)$$

It can be seen that the energy attenuation function of tunnel blasting is different from that of shaft blasting, and the energy attenuation coefficient of

the shaft is approximate twice the at of the tunnel, indicating that seismic wave propagation has an elevation amplification effect. The blasting energy is consumed more rapidly in the vicinity of shaft blasting, and the energy is also consumed more rapidly during the propagation process. This is related to the different excavation methods and ground stress conditions under the two working conditions. The differences between the blasting vibration and rock damage law in the shaft blasting process and the tunnel cannot be ignored.

5 Conclusion

In this paper, the shaft blasting vibration signal is studied from the perspective of the blasting vibration energy distribution characteristics, and the impact of shaft blasting on the surrounding rock and structure is explored, in order to control the blasting hazard through the vibration signal energy distribution characteristics, and the following conclusions can be drawn:

(1) Through wavelet analysis, it is found that the main frequency band of shaft blasting vibration signals is distributed within 0–300 Hz. The ratios of the energy in the 0–300 Hz frequency band of vibration speed in the three directions of x, y, and z to the total energy in each direction are 98.90%, 98.70%, and 99.10%. The vibration energy in the z direction accounts for the most, accounting for 67.95% of the total blasting vibration energy.

(2) The energy peaks of the blasting vibration in the three directions all appear in the frequency range of 0-30 Hz, and the energy peak value in the z direction closest to the explosion source is the largest at 356 cm^2/s^2. The average proportion of energy within the frequency range of 0–30 Hz at 25 m, 31 m, and 41 m from the explosion source is 86.21%, 49.67%, and 39.10%. The energy is concentrated in the low frequency band, which is not conducive to the safety of structures. It is necessary to adjust the blasting plan to make the energy distribution uniform and tend to the high frequency band.

(3) Through the regression analysis of the vibration velocity and energy data of the vertical excavation blasting of the shaft, it is found that the

relationship between the energy and velocity attenuation coefficient is different from that of the tunnel. The energy attenuation coefficient α of the vertical shaft is greater than the energy attenuation coefficient of the tunnel, indicating that the elevation has a significant amplification effect on the blasting vibration energy. In addition, different excavation methods and ground stress are also factors that cause differences to be considered.

Data availability The data are available and explained in this article, while readers can access the data supporting the conclusions of this study.

Declarations

Conflict of interest The authors declare no competing interests.

References

Afum BO, Temeng VA (2015) Reducing drill and blast cost through blast optimisation–a case study. Ghana Mining J 15(2):50–57

Agrawal H, Mishra AK (2018) Evaluation of initiating system by measurement of seismic energy dissipation in surface blasting. Arab J Geosci 11:1–12. https://doi.org/10.1007/s12517-018-3683-3

Agrawal A, Choudhary BS, Murthy VMSR (2022) Seismic energy prediction to optimize rock fragmentation: a modified approach. Int J Environ Sci Technol 19(11):11301–11322. https://doi.org/10.1007/s13762-021-03753-w

Ainalis D, Ducarne L, Kaufmann O, Tshibangu JP, Verlinden O, Kouroussis G (2018) Improved analysis of ground vibrations produced by man-made sources. Sci Total Environ 616:517–530. https://doi.org/10.1016/j.scitotenv.2017.10.291

Baumgart J, Fritzsche C, Marburg S (2022) Infrasound of a wind turbine reanalyzed as power spectrum and power spectral density. J Sound Vib 533:116310. https://doi.org/10.1016/j.jsv.2021.116310

Chen G, Li QY, Li DQ, Wu ZY, Liu Y (2019) Main frequency band of blast vibration signal based on wavelet packet transform. Appl Math Modell 74:569–585. https://doi.org/10.1016/j.apm.2019.05.005

Cong HY, Bi MS, Bi Y, Li YC, Jiang HP, Gao W (2021) Experimental studies on the smoke extraction performance by different types of ventilation shafts in extra-long road tunnel fires. Tunnell Undergr Space Technol 115:104029. https://doi.org/10.1016/j.tust.2021.104029

Ding C, Yang RS, Zheng CD, Yang LY, He SL, Feng C (2021) Numerical analysis of deep hole multi-stage cut blasting of vertical shaft using a continuum-based discrete element method. Arab J Geosci 14(12):1086. https://doi.org/10.1007/s12517-021-07425-4

Huang LZ, Bohne RA, Bruland A, Jakobsen PD, Lohne J (2015) Environmental impact of drill and blast tunnelling: life cycle assessment. J Clean Prod 86:110–117. https://doi.org/10.1016/jjclepro.2014.08.083

Huang D, Cui S, Li XQ (2019) Wavelet packet analysis of blasting vibration signal of mountain tunnel. Soil Dyn Earthq Eng 117:72–80. https://doi.org/10.1016/j.soildyn.2018.11.025

Jing F, Zhang C, Si W, Wang Y, Jiao S (2018) Polynomial phase estimation based on adaptive short-time Fourier transform. Sensors 18(2):568. https://doi.org/10.3390/s18020568

Khademian Z, Ozbay U (2019) Modeling violent rock failures in tunneling and shaft boring based on energy balance calculations. Tunnell Undergr Space Technol 90:62–75. https://doi.org/10.1016/j.tust.2019.04.018

Khodja MEA, Aimer AF, Boudinar AH, Benouzza N, Bendiabdellah A (2019) Bearing fault diagnosis of a PWM inverter fed-induction motor using an improved short time Fourier transform. J Electr Eng Technol 14:1201–1210. https://doi.org/10.1007/s42835-019-00096-y

Li JK, Wang DJ, Fan YB (2014) Blasting vibration damping design and effect analysis in subway shaft construction. Appl Mech Mater 501:1846–1849. https://doi.org/10.4028/www.scientific.net/AMM.501-504.1846

Li XP, Lv JL, Luo Y, Liu TT (2018) Mechanism study on elevation effect of blast wave propagation in high side wall of deep underground powerhouse. Shock Vibr. https://doi.org/10.1155/2018/4951948

Libal U, Spyra K (2014) Wavelet based shock wave and muzzle blast classification for different supersonic projectiles. Expert Syst Appl 41(11):5097–5104. https://doi.org/10.1016/j.eswa.2014.02.037

Ling T, Li S, Liu D, Liang S (2023) Blasting damage of tunnel rock mass based on cumulative effect. Rock Mech Rock Eng 56:1679–1695. https://doi.org/10.1007/s00603-022-03128-8

Ma XM, Wang Y, Lin TS, Yang LY (2021) Intelligent decision system for vertical shaft blasting scheme based on knowledge base and its application. IEEE Access 9:163831–163842. https://doi.org/10.1109/ACCESS.2021.3128550

Ma C, Ran X, Xu W, Yan W, Li T, Dai K, Wan J, Lin Y, Tong K (2023) Fine classification method for massive microseismic signals based on short-time Fourier transform and deep learning. Remote Sens 15(2):502. https://doi.org/10.3390/rs15020502

Maher SP, Matoza RS, Jolly A, de Groot-Hedlin C, Gee KL, Fee D, Iezzi AM (2022) Evidence for near-source nonlinear propagation of volcano infrasound from Strombolian explosions at Yasur Volcano. Vanuatu Bull Volcanol 84(4):41. https://doi.org/10.1007/s00445-022-01552-w

Mehboob S, Khan QUZ, Ahmad S, Anwar SM (2022) Health assessment of RC building subjected to ambient excitation: strategy and application. Earthq Struct 22(2):185–201. https://doi.org/10.12989/eas.2022.22.2.185

Pak TU, Jo GR, Han UC (2022) Prediction of characteristic blast-induced vibration frequency during underground excavation by using wavelet transform. Front Struct Civ Eng 16:1–11. https://doi.org/10.1007/s11709-022-0861-x

Pomasoncco-Najarro A, Trujillo-Valerio C, Arauzo-Gallardo L, Raymundo C, Quispe G, Dominguez F (2022) Pre-split blasting design to reduce costs and improve safety in underground mining. Energy Rep 8:1208–1225. https://doi.org/10.1016/j.egyr.2022.07.109

Robustelli U, Pugliano G (2018) GNSS code multipath short-time Fourier transform analysis. Navig J Inst NaviG 65(3):353–362. https://doi.org/10.1002/navi.247

Schimmack M, Mercorelli P (2019) A structural property of the wavelet packet transform method to localise incoherency of a signal. J Franklin Inst 356(16):10123–10137. https://doi.org/10.1016/j.jfranklin.2019.08.023

Shan RL, Song YW, Bai Y, Zhang LZ, Zhou T, Zhang SP (2018) Research on the energy attenuation characteristics of blasting vibration signals based on wavelet packet transformation. J Min Sci Technol 3(2):119–128. https://doi.org/10.13225/j.cnki.Jccs.2015.1526

Shi CL, Li J, Xu X (2021) Full-scale tests on smoke temperature distribution in long-large subway tunnels with longitudinal mechanical ventilation. Tunnell Undergr Space Technol 109:103784. https://doi.org/10.1016/j.tust.2020.103784

Song YW (2019) Study on the effect on shotcrete and mid-rock caused by reconstruction and expansion blasting of Heiyu tunnel. Dissertation, China University of Mining

Tian XX, Song ZP, Wang JB (2019) Study on the propagation law of tunnel blasting vibration in stratum and blasting vibration reduction technology. Soil Dyn Earthq Eng 126:105813. https://doi.org/10.1016/j.soildyn.2019.105813

Tyrtaiou M, Elenas A (2020) Seismic damage potential described by intensity parameters based on Hilbert-Huang transform analysis and fundamental frequency of structures. Earthq Struct 18(4):507–517. https://doi.org/10.12989/eas.2020.18.4.507

Wang X, Li J, Zhao X, Liang Y (2022) Propagation characteristics and prediction of blast-induced vibration on closely spaced rock tunnels. Tunnell Undergr Space Technol 123:104416. https://doi.org/10.1016/j.tust.2022.104416

Wang YD, Du PX, Chen YY, Hua SH, Wang J, Shi C, Liu K (2023) Mixed ventilation approach combined with single-shaft complementary system for highway tunnels. Tunnell Under Space Technol 132:104927. https://doi.org/10.1016/j.tust.2022.104927

Wenbin G, Chen JH, Wang ZX, Wang ZH, Liu JQ, Lu M (2015) Experimental study on the measurement of water bottom vibration induced by underwater drilling blasting. Shock Vib 2015:1–8. https://doi.org/10.1155/2015/496120

Wu J, Wu L, Sun M, Lu YN, Han YH (2022a) Analysis and research on blasting network delay of deep-buried diversion tunnel crossing fault zone based on EP-CEEMDAN-INHT. Geotech Geol Eng 40(3):1363–1372. https://doi.org/10.1007/s10706-021-01968-9

Wu YY, Mu CM, Zong Q, Wu JH, Zhou H (2022b) Study on blasting vibration control of brick-concrete structure under subway tunnel. Appl Sci 12(21):10960. https://doi.org/10.3390/app122110960

Xie LD, Dong ZX, Qi YJ, Qiu RH, He Q (2019) Vibration failure of young low-temperature concrete shaft linings caused by blasting excavation. Adv Civ Eng 2019:1–10. https://doi.org/10.1155/2019/5343618

Xie HP, Zhang K, Zhou CT, Wang JX, Peng Q, Guo J, Zhu JB (2022) Dynamic response of rock mass subjected to blasting disturbance during tunnel shaft excavation: a field study. Geomech Geophys Geo-Energy Geo-Resour 8(2):52. https://doi.org/10.1007/s40948-022-00358-6

Xu C, Deng CF (2016) Investigating spectral behavior of tunnel blast-induced vibration using wavelet analysis: a case study of a dam in China. J Civ Struct Heal Monit 6:637–647. https://doi.org/10.1007/s13349-016-0183-6

Xue W, Yao Z, Cheng H, Rong C (2016) Blasting vibration on deep shaft ingate rock damage and its control measures. J Vibroeng 18(3):1639–1653

Yang LY, Chen SY, Dong PX, Wang QC, Huang C (2020) Orthogonal analysis and numerical simulation of rock mechanics parameters in stress field of shaft heading face. Adv Mater Sci Eng 2020:1–11. https://doi.org/10.1155/2020/3107364

Yao YZ, Zhang SG, Shi L, Cheng XD (2019) Full-scale tests on smoke temperature distribution in long-large subway tunnels with longitudinal mechanical ventilation. Tunn Undergr Space Technol 28(1):77–87. https://doi.org/10.1177/1420326X17734906

Zhang ZQ, Zhang H, Tan YJ, Yang HY (2018) Natural wind utilization in the vertical shaft of a super-long highway tunnel and its energy saving effect. Build Environ 145:140–152. https://doi.org/10.1016/j.buildenv.2018.08.062

Zhang SH, Gao WX, Yan L, Liu JC, Liu LS (2020) The characteristics of blasting vibration frequency bands in jointed rock mass slope. Environ Earth Sci 79:1–17. https://doi.org/10.1007/s12665-020-09267-x

Zhong GS, Xu GY, Xiong ZB (2006) Application research of blasting seismic signal energy analysis method based on wavelet transform. Explos Shock Waves 26(3):222–227